Virus Research 199 (2015) 9–19

Contents lists available at ScienceDirect

Virus Research

journal homepage: www.elsevier.com/locate/virusres

Identification of morphological differences between avian influenza A viruses grown in chicken and duck cells

Firas Al-Mubarak[a,b], Janet Daly[a], Denise Christie[c], Donna Fountain[a], Stephen P. Dunham[a,*]

[a] School of Veterinary Medicine and Science, University of Nottingham, Sutton Bonington Campus, Leicestershire, College Road, Loughborough LE12 5RD, UK
[b] Department of Microbiology – Virology, College of Veterinary Medicine and Science, Basra University, Iraq
[c] School of Life Sciences, The University of Nottingham, Queen's Medical Centre, Nottingham NG7 2UH, UK

ARTICLE INFO

Article history:
Received 27 July 2014
Received in revised form
11 December 2014
Accepted 10 January 2015
Available online 19 January 2015

Keywords:
Avian influenza virus
Chicken
Duck
Virus morphology
Filamentous virus

ABSTRACT

Although wild ducks are considered to be the major reservoirs for most influenza A virus subtypes, they are typically resistant to the effects of the infection. In contrast, certain influenza viruses may be highly pathogenic in other avian hosts such as chickens and turkeys, causing severe illness and death. Following *in vitro* infection of chicken and duck embryo fibroblasts (CEF and DEF) with low pathogenic avian influenza (LPAI) viruses, duck cells die more rapidly and produce fewer infectious virions than chicken cells. In the current study, the morphology of viruses produced from CEF and DEF cells infected with low pathogenic avian H2N3 was examined. Transmission electron microscopy showed that viruses budding from duck cells were elongated, while chicken cells produced mostly spherical virions; similar differences were observed in viral supernatants. Sequencing of the influenza genome of chicken- and duck-derived H2N3 LPAI revealed no differences, implicating host cell determinants as responsible for differences in virus morphology. Both DEF and CEF cells produced filamentous virions of equine H3N8 (where virus morphology is determined by the matrix gene). DEF cells produced filamentous or short filament virions of equine H3N8 and avian H2N3, respectively, even after actin disruption with cytochalasin D. These findings suggest that cellular factors other than actin are responsible for the formation of filamentous virions in DEF cells. The formation of elongated virions in duck cells may account for the reduced number of infectious virions produced and could have implications for virus transmission or maintenance in the reservoir host.

1. Introduction

Influenza A viruses show variable morphology, with shapes ranging from spherical or elliptical and about 100 nm in diameter to elongated or filamentous with a length reaching to more than several micrometres; occasionally, they are pleomorphic (Calder et al., 2010). Viruses have three membrane-associated proteins: haemagglutinin (HA); neuraminidase (NA); and a small amount of matrix protein 2 (M2). Beneath the lipid envelope, there is a matrix protein 1 (M1) layer. All these proteins play an important role in virus morphogenesis (Bouvier and Palese, 2008; Palese and Shaw, 2007). Diversity of virus morphology is thought to be a genetic trait; in particular the seventh viral RNA segment (M), which encodes the matrix proteins, plays a dominant role in determining virus shape (Elleman and Barclay, 2004; Roberts et al., 1998). However, the importance of specific M protein residues as determinants of virus morphology appears to differ between influenza viruses of different species (Elton et al., 2013). In addition, the surface glycoproteins (HA and NA) have also been implicated in modulation of virus shape (Jin et al., 1997; Zhang et al., 2000).

Non-viral factors may also determine influenza A virus morphology. Newly isolated clinical strains usually comprise filamentous forms, while laboratory-adapted viruses, especially with many

Abbreviations: 293T, human embryonic kidney cells; BSA, bovine serum albumin; cDNA, complementary deoxyribonucleic acid; CEF, chicken embryo fibroblasts; Cyt.D, cytochalasin D; DAPI, 4′,6-diamidino-2-phenylindole; DEF, duck embryo fibroblasts; DM, dissociation medium; DMEM, Dulbecco's modified Eagle's medium; EM, electron microscopy; FCS, foetal calf serum; HA, haemagglutinin; HPAI, highly pathogenic avian influenza; HRP, horseradish peroxidase; LC3, microtubule-associated protein 1A/1B-light chain 3; LLC-MK2, rhesus monkey kidney epithelial cell line; LPAI, low pathogenic avian influenza; M, matrix; MDCK, Madin Darby canine kidney cells; MOI, multiplicity of infection; NA, neuraminidase; NP, nucleoprotein; PBS, phosphate buffered saline; PCR, polymerase chain reaction; RNA, ribonucleic acid; RT-PCR, reverse transcription-polymerase chain reaction; SDS, sodium dodecyl sulphate; TCPK, L-1-tosylamido-2-phenylethyle chloromethyl ketone; VLPs, virus-like particles.

* Corresponding author. Tel.: +44 115 95 16580; fax: +44 115 95 16440.
E-mail address: stephen.dunham@nottingham.ac.uk (S.P. Dunham).

http://dx.doi.org/10.1016/j.virusres.2015.01.005

passages in eggs or cell culture, typically exhibit spherical morphology (Cox et al., 1980). Cellular factors such as cell polarity and the actin cytoskeleton can play a major role in determining virus morphology (Sun and Whittaker, 2007). Epithelial cells have been shown to produce more filamentous particles than fibroblasts and an intact actin cytoskeleton is important for forming filamentous but not spherical virions (Roberts and Compans, 1998; Simpson-Holley et al., 2002). Furthermore, endocytic trafficking regulator and its effector Rab11-family interacting protein 3 (Rab11-FIP3) are also required to support the formation of filamentous virions (Bruce et al., 2010).

Aquatic birds such as ducks are considered to be the major natural reservoirs of influenza A viruses (Webster et al., 1992). Infection of ducks is usually clinically silent, and virus replication mainly occurs in the epithelial cells of the digestive tract. Large amount of viruses are shed in faeces leading to environmental contamination (Webster et al., 1978). In contrast, when transmitted to domestic poultry such as chickens, turkeys and quail, low pathogenic avian influenza (LPAI) viruses typically cause mild respiratory signs and reduced productivity (Pillai et al., 2010). In addition, in experimentally infected ducks, most highly pathogenic avian influenza (HPAI) virus infections are non-lethal and produce limited or no clinical signs (Kishida et al., 2005; Jeong et al., 2009; Shortridge et al., 1998). In contrast, HPAI viruses infecting chickens (naturally and experimentally) are lethal causing mortality reaching 100%, often within two days. Kuchipudi et al. (2011) observed that duck cells undergo rapid cell death following *in vitro* infection with LPAI H2N3 viruses, while cell death occurs less rapidly after infection in chicken cells. This study also showed that the number of infectious virions produced in chicken cells was significantly higher than in duck cells. However, there was no significant difference between viral M gene RNA production between the two species. We hypothesized that the differences in production of infectious H2N3 virus in chicken and duck cells may be due to altered virus assembly or defects in the viral structure. We therefore examined virus production from chicken and duck cells using transmission electron microscopy and compared the ability of cells to produce filamentous virus after infection with low pathogenic avian H2N3 (which typically has a spherical morphology in cell culture) or a filamentous equine virus, H3N8 (where the M protein sequence determines a filamentous morphology) by immunofluorescence. Additionally, the importance of cellular actin in determining virus morphology was investigated by disruption with cytochalasin D.

2. Materials and methods

2.1. Viruses

Two influenza A subtypes were used in this study: LPAI H2N3 (A/mallard duck/England/7277/06) and equine influenza H3N8 (A/equine/Newmarket/5/03) that were kindly provided by Dr. Ian Brown (Animal and Plant Health Agency) and Dr. Debra Elton (Animal Health Trust), respectively. H3N8 has a filamentous morphology determined largely by amino acid 85 (S) and 231 (D) of the M protein (Elton et al., 2013). Viruses were propagated in the allantoic cavity of embryonated hen's eggs.

2.2. Cells

MDCK cells were maintained in growth media consisting of Dulbecco's modified Eagle's medium containing 10% foetal calf serum (FCS; Invitrogen) and supplemented with 100 U/ml penicillin and 100 μg/ml streptomycin (Invitrogen). Embryo fibroblast cells were extracted from 8-day-old chicken embryos (eggs provided by Henry Stewart & Co. Ltd., Louth, Lincs, UK) and 10.5-day-old Pekin duck embryos (eggs provided by Cherry Valley Farms Ltd., Rothwell, Lincs, UK). The embryos were minced and digested in 0.25% trypsin in dissociation medium (DM; F12 Hams, 100 U/ml penicillin, 100 μg/ml streptomycin, 1.5% amphotericin B) at 37 °C for 1 h. Large undigested tissue pieces were removed using a cell strainer and the remaining suspension was centrifuged at 400 × *g* for 5 min. Cells were seeded into cell culture flasks (Nunc) and maintained in growth media.

2.3. Infection of chicken and duck cells

Monolayers of chicken and duck embryo fibroblast cells were grown in 24-well plates. Cells were infected with LPAI H2N3 in triplicate at multiplicity of infection (MOI) of 1.0 in serum-free medium (infection medium) supplemented with 2% Ultroser G (Pall Biosepra), 100 U/ml penicillin and 100 μg/ml streptomycin (Invitrogen), and 500 ng/ml TPCK trypsin (Sigma–Aldrich), and incubated for 2 h. After 2 h, the cells were carefully washed three times with PBS, to remove residual virus inoculum, followed by addition of fresh media. Supernatants were collected at 2, 4, 6, 8, 24, and 48 h post infection and were stored at −80 °C until use.

2.4. Virus infectivity assay

Confluent MDCK cells grown in 96-well plates were infected in triplicate with virus collected from chicken and duck cells to determine virus infectivity. Cells were washed after 2 h incubation with virus, incubated for a further 4 h and then fixed with 1:1 acetone:methanol. Viral nucleoprotein expression was detected using a primary mouse monoclonal antibody (Abcam, Cambridge, UK) followed by visualization with Envision+ HRP (DAB; Dako, Ely, UK). Cells expressing viral nucleoprotein were counted and the mean number of positive cells in four fields used to calculate focus-forming units of virus per microlitre of inoculum.

2.5. Quantification of virus production (measurement of M gene copy number)

A one-step reverse transcription-RT-PCR assay using influenza virus M gene-specific PCR primers and hydrolysis probe was performed as previously described (Slomka et al., 2009). In brief, viral RNA was extracted from culture supernatants of infected chicken and duck cells using QIAamp viral RNA purification kit (Qiagen) following the manufacturer's instructions. A one-step absolute quantification of viral M gene expression was performed using SuperScript® III Platinum® One-Step qRT-PCR Kit (Invitrogen). Quantitative RT-PCR conditions and cycling parameters for samples were as follows: one cycle at 50 °C for 30 min, one cycle at 95 °C for 2 min, and 40 cycles of 95 °C for 15 s and 60 °C for 1 min. Threshold cycle (Ct) values were converted to viral gene copy number by a standard curve generated using *in vitro* transcribed M gene RNA using LightCycler 480 software, release 1.5.0 (Roche).

2.6. Western blotting

Polyacrylamide gel electrophoresis using Novex 14% Tris–Glycine mini gels (Invitrogen), followed by western blotting, were used to detect M1 protein in culture supernatants. Samples to be tested, 1 μl of chicken or duck virus supernatant, were suspended in 5 μl of 2× Tris glycine SDS sample buffer (Invitrogen) with 1 μl of 2× reducing agent (Invitrogen) and distilled water (to 10 μl) to lyse viral protein. The mixture was incubated at 95 °C for 5 min, and then cooled and spun briefly. Samples were run on the gel for approximately 1 h then transferred to a 0.2 μm Hybond ECL Nitrocellulose Membrane (GE Healthcare, Life Sciences) by wet blotting. The membrane was treated with

blocking buffer (5% skimmed dried milk in 1× TBS) for 50 min at room temperature with gentle shaking, and then incubated with a mouse monoclonal antibody to influenza M1 protein (ABD Serotec) overnight at 4 °C. The membranes were incubated with HRP-linked anti-mouse IgG antibody (Cell Signalling Technology) for 1 h at room temperature and then subjected to ECL prime reagent (GE Healthcare, Life Sciences) to detect the antigen–antibody complexes. The amount of protein production was determined by optical densitometry using Image J 1.47 software.

2.7. Transmission electron microscopy

CEF and DEF cells were grown on Thermanox plastic coverslips (Nunc) in 24-well plates. The cells were infected with H2N3 in serum-free infection media at an MOI of 1.0 for 7 h. They were then fixed with EM fixative buffers (3% glutaraldehyde in 0.1 M sodium cacodylate buffer). After two rinses in 0.1 M cacodylate buffer (pH 7.2), samples were placed in 1% osmium tetroxide in the same buffer for 1hr, then rinsed in distilled water for 5 min. They were subsequently dehydrated in graded ethanol series, culminating in two changes in propylene oxide. The samples were then infiltrated, polymerized with resin and sectioned. They were stained with ethanolic urenyle acetate followed by lead acetate and examined using a Tecnai bio twin digital transmission electron microscope run at 100 Kv.

To observe viruses from culture supernatants, cells were infected with the virus in T75 flasks at an MOI of 1.0 for 24 h. Supernatants were then harvested, clarified by centrifugation at 500 × *g* for 10 min, and concentrated by Amicon® Ultra 100 K NMWL (National Molecular Weight Limit) Centrifugal Filter Device (Millipore) at 3000 × *g* for 30 min. They were then pipetted onto a Formvar coated copper grid, negatively stained with 2% phosphotungstic acid, and examined under the electron microscope.

2.8. Polymerase chain reaction and sequencing

Extraction of viral RNA from chicken and duck culture supernatants was performed using a QIAamp viral RNA purification kit (Qiagen) following the manufacturer's instructions. Amplification of each gene segment of influenza virus was performed using One-Step Super Script III RT-PCR kit (Invitrogen). Two or more sets of primers were designed for each gene to amplify and sequence the whole genome (primer details and PCR conditions can be provided on request). PCR products were then cleaned up using QIAquick PCR purification kit (Qiagen) according to manufacturer's instructions and sent to Source BioScience for sequencing. The sequences were edited using Chromas Lite software and then were assembled and aligned by Geneious Inspirational Software for Biologists (www.geneious.com).

2.9. Immunofluorescence

MDCK, CEF and DEF cells were grown on glass coverslips (19 mm diameter) in 12-well plates, and incubated overnight at 37 °C. The cells were then infected either with the filamentous virus strain (H3N8) or with the non-filamentous strain (H2N3) in infection medium at an MOI of 1.0 for 2 h. Cells were then washed three times with PBS and fresh medium was added either with cytochalasin D (5 μg/ml or 0.5 μg/ml) or without, and further incubated for 6 h at 37 °C. Cells were washed with PBS, incubated with 4% paraformaldehyde for 10 min, and then rinsed with PBS. Cells were blocked with 1% bovine serum albumin (Fisher Scientific, UK) for 1 h at room temperature and incubated with polyclonal antibody specific to the H2 antigen (chicken H2N3 antiserum, a kind gift from Dr. Ian Brown, Animal and Plant Health Agency, UK) or specific to the H3 antigen (rabbit H3N8 antiserum, a kind gift from Dr. Debra Elton, Animal Health Trust, UK) for 1 h at room temperature. Cells were then washed three times in PBS, for 5 min each, before incubating in the dark for 1 h at room temperature with a secondary antibody (either with goat anti-chicken or anti-rabbit IgG antibody, Invitrogen) labelled with green fluorescent Alexa Fluor® 488. After washing, cells were incubated in the dark for 1 h with Alexa Fluor® 546 Phalloidin (Invitrogen) to stain filamentous (F-)actin. Cells were then washed, allowed to air dry, and mounted with Prolong Gold Anti-Fade Reagent with 4′,6-diamidino-2-phenylindole (DAPI; Invitrogen) and viewed using a Leica DM 5000B epifluorescence imaging system.

2.10. Statistical analysis

All data were analyzed using GraphPad Prism software, version 6.02. Comparisons of M gene and protein expression between chicken and duck grown viruses were made using Student's *t* test. Infectious virus production from chicken and duck cells was analyzed using two-way ANOVA.

3. Results

3.1. H2N3 virus replication in chicken and duck cells

Virus replication following infection of chicken and duck cells was measured at 2–48 h post infection (pi) by titration of infectious virus using a focus forming assay in MDCK cells. Virus production was comparable between species up to 8 h pi, but after 24 h and 48 h pi there was a significant difference in virus production between species, with chicken cells producing 4–5 fold more virus than duck cells (Fig. 1a). Replication of H2N3 virus in chicken and duck cells was confirmed by measuring M1 gene RNA and protein expression following cell infection with the virus for 8 and 24 h, using quantitative real-time PCR and western blotting, respectively. There was no significant difference ($p > 0.05$) between the level of M gene (Fig. 1b and c) and M protein (Fig. 2), at either 8 h or 24 h, in chicken and duck cell grown viruses (Figs. 1 and 2).

3.2. EM imaging of infected chicken and duck cells with H2N3

EM showed clear differences in the morphology of virions budding from chicken or duck cells. The majority of viruses budding from chicken cells were spherical and about 100 nm in diameter, while the majority of viruses budding from infected duck cells were elongated to filamentous ranging in size from 500 nm to a few micrometres (Fig. 3).

To achieve a further overview of the variations in virion morphology, concentrated viruses from culture supernatants of infected chicken and duck cells were examined under the electron microscope at different magnifications (Fig. 4). Morphological differences were clearly observed between the two species. Viruses derived from chicken cells were typically spherical while those obtained from duck cells were elongated to pleomorphic with sizes similar to those budding from cells.

3.3. Sequencing of H2N3 virus derived from duck and chicken cells

To determine whether virus mutations might be responsible for the observed differences in virus morphology between species, all viral genes were amplified by using one step RT-PCR and then directly sequenced. The H2N3 stock virus used to infect the cells and the chicken and duck progeny viruses were sequenced. Each of the eight viral genes was amplified using one or more sets of primers in order to cover the whole genome. The nucleotide sequences of progeny viruses produced from both duck and chicken fibroblasts

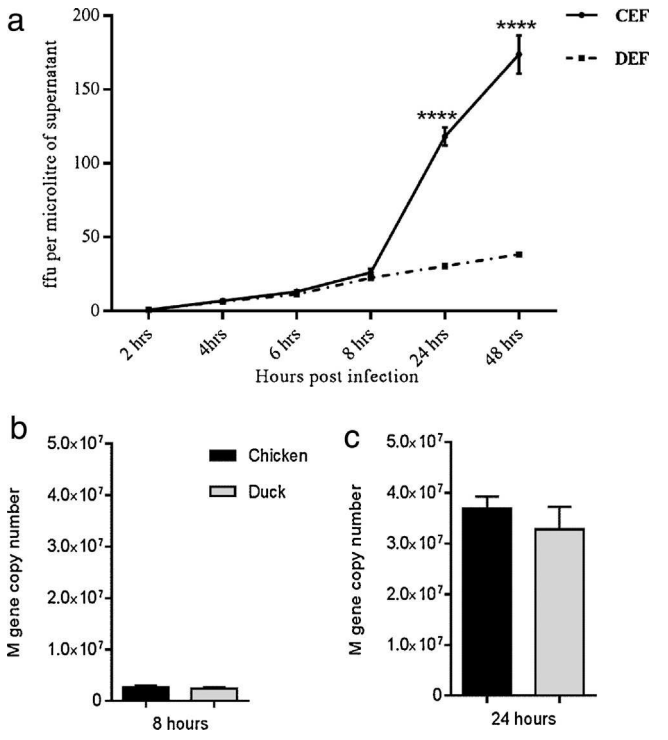

Fig. 1. Replication of influenza A H2N3 in chicken and duck cells. Infectious virus titre in supernatants collected from chicken embryo fibroblasts (CEF; solid line) and duck embryo fibroblasts (DEF; dash-dot line) from 2 to 48 h post infection measured by focus forming assay on MDCK cells (A). Significant differences ($p < 0.0001$; ****) in the level of infectious virus production were observed between species at 24 and 48 h post infection (ffu: focus forming units). Matrix gene production in culture supernatants of chicken cells (black bars) and duck cells (grey bars) infected with avian H2N3 for 8 h (B) and 24 h (C). There was no significant difference in M gene production between hosts at the two time points ($p > 0.05$). Data shown represent the mean of triplicate wells with error bars showing standard deviation (SD).

was identical in all eight gene segments to the H2N3 virus that was used to infect the cells.

3.4. Virus morphology in the presence and absence of an inhibitor of actin polymerization

We then sought to determine whether the actin cytoskeleton might be responsible for the formation of filamentous viruses in duck cells, by examining virus HA and cellular actin using fluorescent microscopy. Cells were infected with either H3N8 (Figs. 5 and 6) or H2N3 (Figs. 7 and 8) in the absence or presence of cytochalasin D, a chemical inhibitor of actin polymerization. Images were taken of green (Alexa 488) fluorescent antibody stained viral HA (H2 or H3), filamentous (F-)actin was stained with phalloidin and then images were merged with DAPI (blue) images to visualize cell nuclei. Cytochalasin D was pre-titrated to determine the dose of drug (0.5 μg/ml) required to be sufficient to disrupt actin without causing complete collapse of the actin cytoskeleton and rounding of the cells. As expected, mock-infected cells showed very low levels of non-specific anti-HA antibody binding. The phalloidin-stained F-actin in untreated mock-infected cells was distributed as a layer underlying the plasma membrane, whereas drug-treated cells showed loss of the cortical actin web, which aggregated in clumps, distributed across the cell (data not shown).

In the absence of cytochalasin D, all cells infected with equine H3N8 produced distinctive HA-stained filamentous structures on the cell surface that reached several microns in length and were distributed regularly on the cell surface (Fig. 5). In the presence of the actin inhibitor, MDCK and CEF cells produced spherical virions, while in the DEF cells, virus morphology changed from elongated to short filaments (Fig. 6). In addition, the viral HA formed clumps in ring-shaped domains surrounding F-actin. These clumps were more marked in MDCK and CEFs than DEFs. Treatment of duck cells with a higher dose of cytochalasin D (5 μg/ml) showed rounding of the cells and actin collapse, but there was no significant reduction in the formation of short filament virions (data not shown). Following infection of MDCK and CEF cells with H2N3,

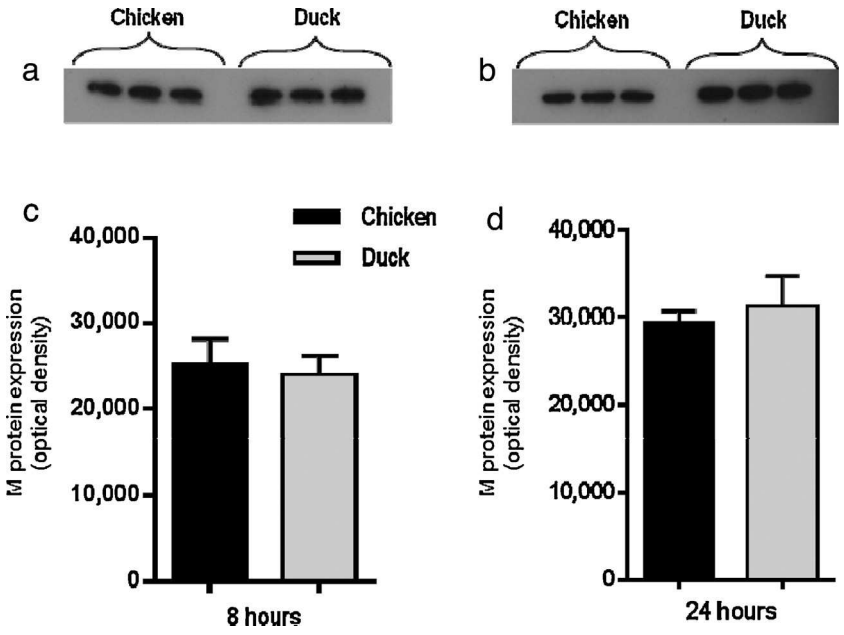

Fig. 2. Western blot analysis of viral matrix protein. Viral protein, extracted from culture supernatants, was subjected to SDS-PAGE. M protein expression from infected chicken and duck cells at 8 h (A), and at 24 h (B). Quantitative analysis showed no difference in M protein expression between chicken (black bars) and duck (grey bars) cells at either time point (C and D; $p > 0.05$). Data shown represent the mean of triplicate wells with error bars showing SD.

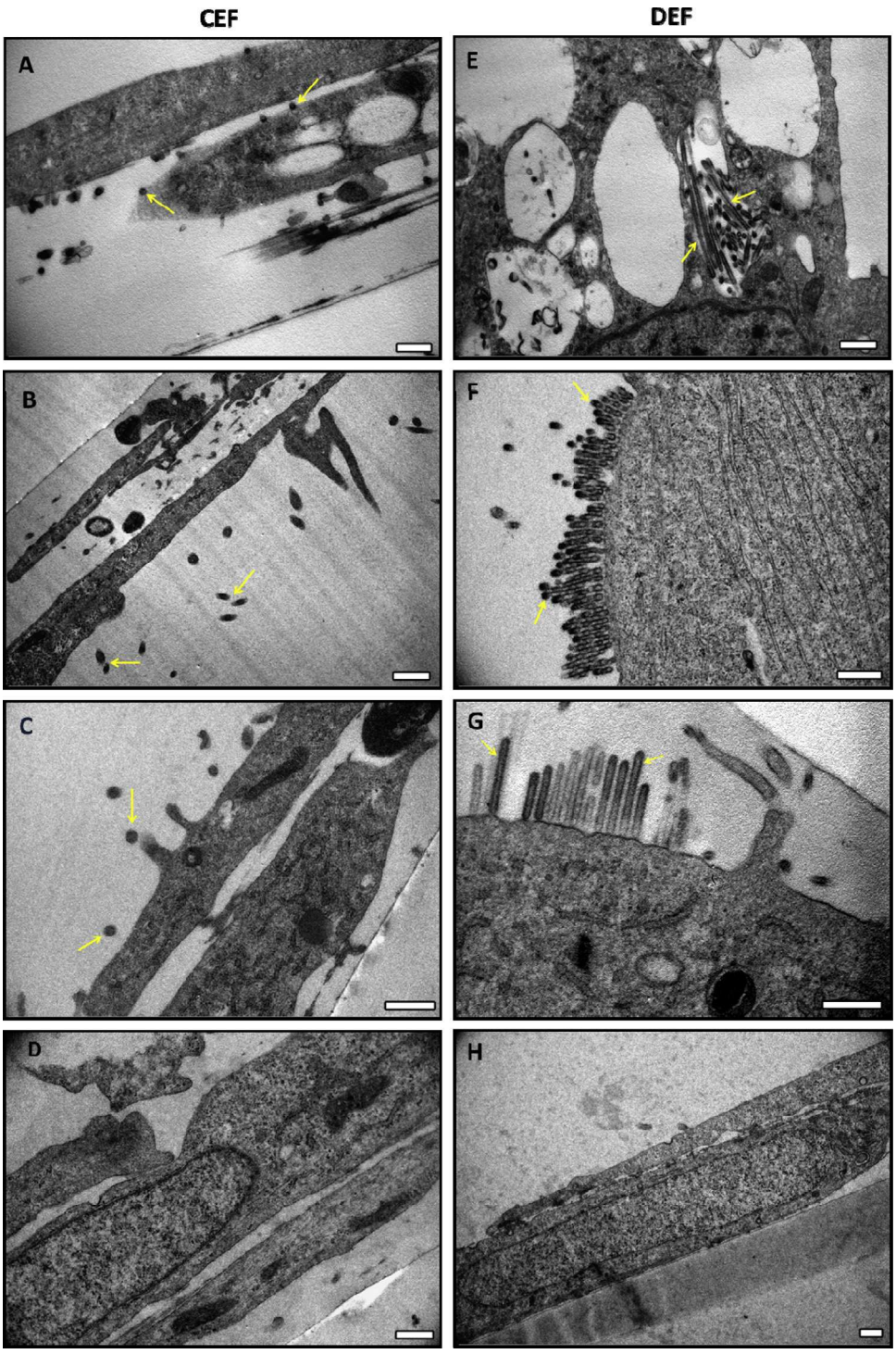

Fig. 3. Budding influenza virus particles from infected CEF and DEF cells. Cells were infected with avian H2N3 at an MOI of 1.0 for 7 h. Electron micrographs show the presence of spherical virions budding from the surface infected chicken fibroblasts (A–C) while most of the budding particles from the surface of duck fibroblasts are elongated or short filaments (E and F) with some filamentous bundles (G; indicated by arrows). Uninfected controls of CEF and DEF cells (D and H, respectively) showed no virions. Scale bar 500 nm.

spherical virions were produced in the absence (Fig. 7) or presence of cytochalasin D (Fig. 8) with no obvious filamentous virus present. Following infection of DEF, striking short filaments were produced in the absence of the drug (Fig. 7) and elongated and pleomorphic structures were produced in the presence of 0.5 μg/ml of the drug (Fig. 8).

4. Discussion

It is well known that influenza A viruses exhibit different morphological structures. Most clinical isolates are predominantly filamentous (Chu et al., 1949), while the laboratory-adapted strains are mostly spherical or elliptical (Kilbourne and Murphy, 1960).

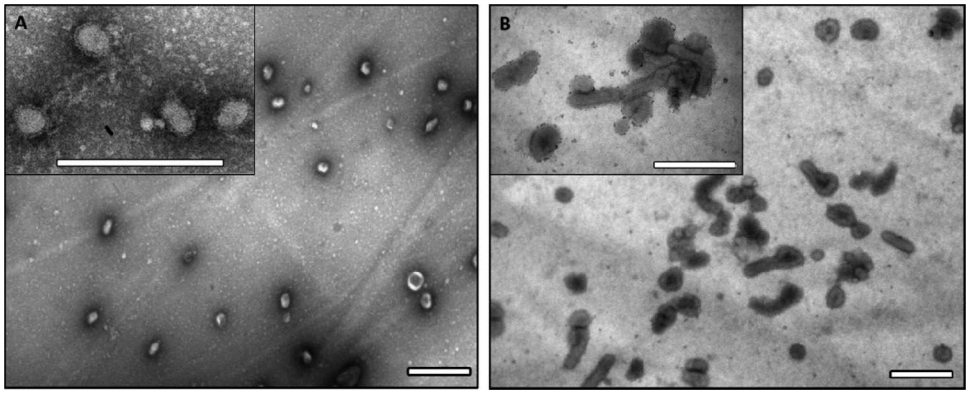

Fig. 4. Electron micrographs of negatively stained virions released from CEF and DEF cells. Spherical particles were detected after imaging culture supernatants of infected chicken cells, while pleomorphic particles were frequently observed after imaging culture supernatants of infected duck cells under electron microscope. Scale bar 500 nm.

It has been shown that the matrix (M gene), which encodes two proteins (M1 and M2), plays a role in modulating filamentous *versus* spherical virus morphology (Hughey et al., 1995; Elleman and Barclay, 2004; Bourmakina and Garcia-Sastre, 2003). In addition, viral morphology, genome packaging, and incorporation of NA and M1 into virions are also reported to be affected by changes in the amino acid sequences (Burleigh et al., 2005) or deletion in the cytoplasmic tails of the other viral transmembrane proteins (HA, NA) (Jin et al., 1997; Zhang et al., 2000). Recently, specific residues in viral nucleoprotein have also been shown to play a critical role in virus morphology (Bialas et al., 2014). However, no mutations or deletions were detected in the consensus sequence of any of the 8 viral gene segments obtained from LPAI grown in chicken or duck cells. This strongly suggests that there are underlying cellular mechanisms present in duck cells that enhance the formation of filamentous virus.

A previous study showed that duck cells undergo rapid cell death following *in vitro* infection with H2N3 viruses, accompanied by a reduced production of infectious virus, 24 and 48 h post infection, while cell death occurs less rapidly after infection in chicken cells (Kuchipudi et al., 2011). However, there was no significant difference between virus RNA output measurements from the two species. In the current study, we measured viral titres at a range of time points post infection (2, 4, 6, 8, 24, and 48 h). Virus titre was similar between chicken and duck grown viruses between 2 and 8 h post infection, but was significantly higher for chicken than duck grown virus at 24 and 48 h post infection, confirming the previous findings (Kuchipudi et al., 2011). In addition, supernatants collected at 8 and 24 h post infection were used to determine viral RNA replication and viral M protein expression. The two time points were selected as a representative of a significant (24 h) and non-significant (8 h) difference in infectious virus production between chicken and duck virions. Although the level of infectious virus production was different between chicken and duck cells, at 24 h post infection, levels of M1 gene replication and protein expression were similar between the hosts. Interestingly, other studies have shown that the production of filamentous influenza virus is correlated with a reduction in infectious virus titre (Bialas et al., 2012; Campbell et al., 2014a,b). There has been much speculation that filamentous viruses may be maintained in clinical isolates because they give the virus an advantage in virus transmission. Further studies of virus morphology in duck cells both *in vitro* and *in vivo* are warranted to enhance our understanding of the importance of virus morphology for maintenance and transmission of the virus in its natural reservoir host.

The matrix protein of influenza A virus has been shown to play a major role in mediating budding of virus-like particles (VLPs) in the absence of other viral proteins (Gomez-Puertas et al., 2000; Latham and Galarza, 2001). In the absence of any significant difference in M gene sequence or expression level between species, further studies are required to determine whether there is any evidence of altered expression of other viral proteins that may affect virus assembly and release, resulting in reduced infectivity of duck grown viruses. Factors such as viral gene mutations or deletions do not appear to be responsible given failure to identify these following sequencing of the virus genome. In addition, defective interfering (DI) particles, which are composed of a normal set of virus proteins but lack a complete viral genome, may be generated during the course of replication. Because they lack the essential genetic information, DI particles are usually non-infectious and non-replicating particles (Holland, 1990). Such kind of particles could be generated from DEFs following infection resulting in production of a low infectious virus titre.

Sample preparation processes may play a role in producing pleomorphic virus particles (Noda, 2011). Studies have shown that pleomorphic morphology is introduced during the storage of virions at 4 °C after they are harvested (Choppin et al., 1961). In addition, virus morphology can be substantially disrupted by ultracentrifugation of non-fixed samples which results in the production of irregular shaped virions (Sugita et al., 2011). To avoid these possibilities, viruses were concentrated using an alternative method based on the filtration of culture supernatants at a lower centrifugation speed that should maintain the virus shape. In addition, non-concentrated viruses were also examined under the electron microscope and no obvious difference to the concentrated samples was observed (data not shown).

Cellular factors such as cell polarity and actin cytoskeleton network are important in determining the production of filamentous virions. Filamentous particles up to 30 μm can be observed on the surface of polarized cells following infection with a filamentous strain such as A/Udorn/72 (H3N2) virus, whereas spherical or slightly elongated particles are usually detected following infection of non-polarized cells (Roberts and Compans, 1998). However, DEF cells used in this study produced short filaments after infection with spherical H2N3 virus whereas CEF cells produced only spherical virions. Despite this, both CEF and DEF cells are capable of producing filamentous particles following the infection with the filamentous strain H3N8. Matrix protein, with S85 and D231 as critical residues, largely determines the morphology of the A/equine/Newmarket/5/03 (H3N8) strain (Elton et al., 2013). The H2N3 virus used in this study differs at M protein residue 85 (S85N), which may contribute to the observed spherical morphology in CEFs. The equine H3N8 prototype strain, Miami/63, also adopts a spherical morphology, again determined by the presence of asparagine at residue 85 (Elton et al., 2013).

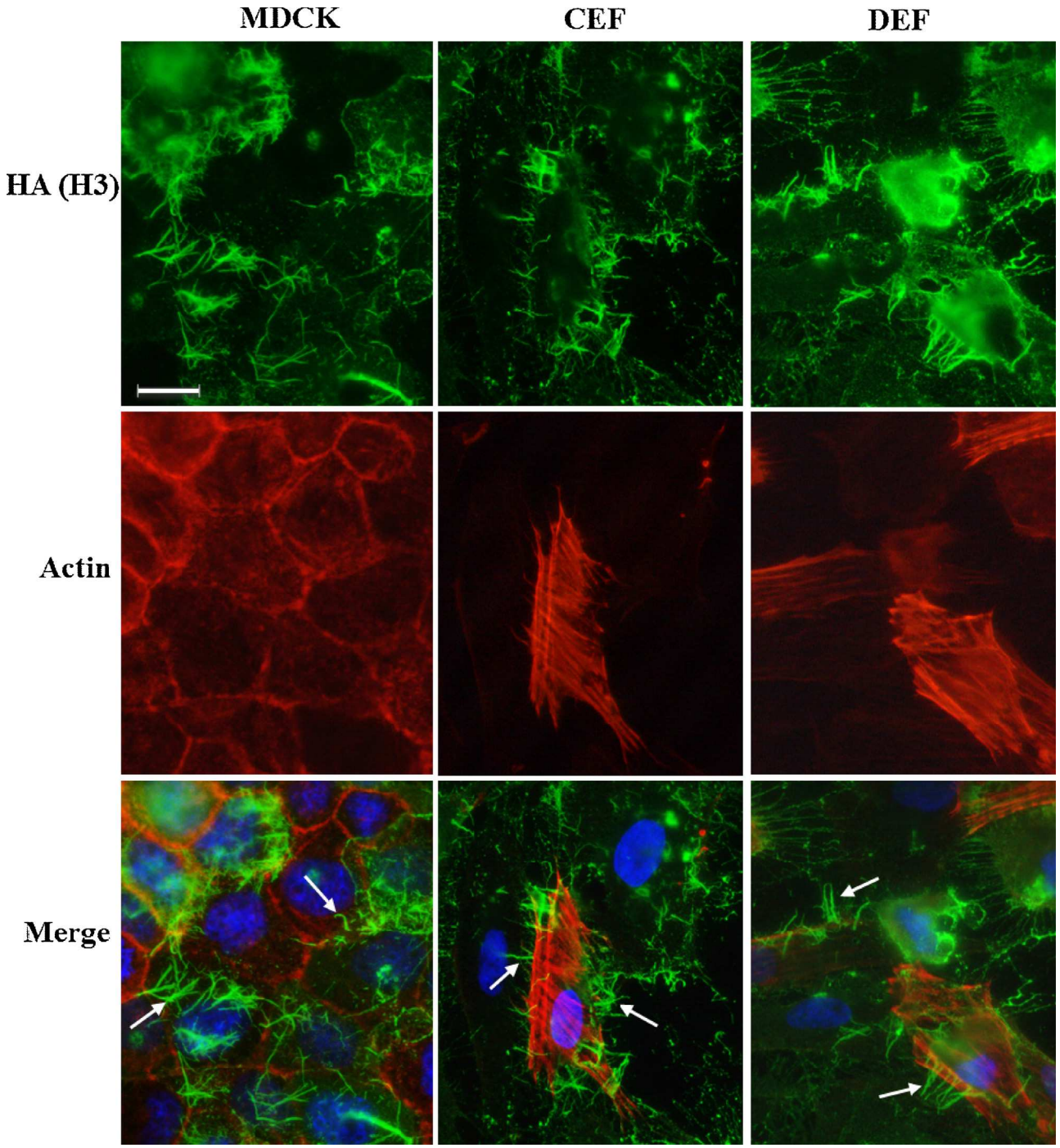

Fig. 5. H3N8 morphology in MDCK, CEF and DEF cells. Cells were infected with virus in the absence of cytochalasin D and stained for surface HA (green), actin (red–orange), and DNA (blue). Filamentous virions were observed on the surface of all cells (indicated by arrows). Scale bar 10 μm. (For interpretation of the references to color in this figure legend, the reader is referred to the web version of this article.)

A number of host cell factors including the actin cytoskeleton have been shown to influence virus morphology. Cytochalasin D prevents actin polymerization by binding to the boarded ends of actin filaments and blocking the addition of soluble (G)-actin monomers (Schliwa, 1982). A previous study showed that cytochalasin D inhibits the production of the filamentous form of A/Udorn/72 (H3N2) virus, but not the spherical A/PR/8/34 (H1N1) virus suggesting that the assembly of filamentous particles requires an intact actin cytoskeleton (Roberts and Compans, 1998). On the other hand, Simpson-Holley et al. (2002) tested the effect of other actin inhibitors, jasplakinolide and latrunculin A, after infecting cells with the filamentous strain A/Udorn/72 (H3N2) and the spherical strain A/PR/8/34 (H1N1). These drugs are mechanistically different inhibitors of actin: jasplakinolide binds to F-actin and inhibits actin depolymerization (Bubb et al., 1994) and latrunculin A inhibits actin polymerization by sequestering G-actin monomers (Coue et al., 1987). These drugs have only been previously used to inhibit the actin cytoskeleton of MDCK cells and all resulted in a marked decrease in filamentous virus production. In the current study, the viral HA formed clumps in ring-shaped domains, which

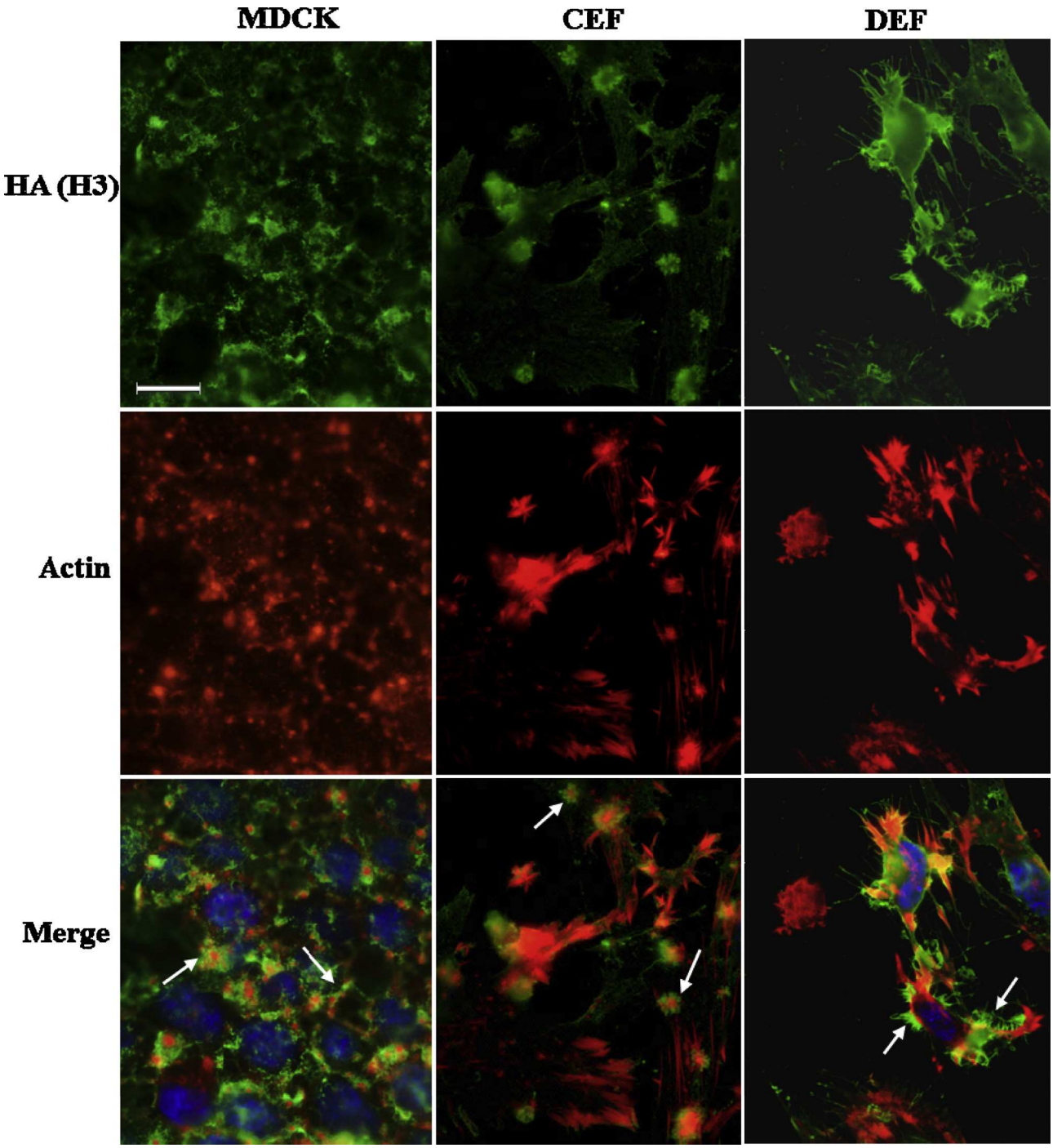

Fig. 6. Differences in H3N8 morphology between MDCK, CEF and DEF cells treated with cytochalasin D. Cells were infected with virus in the presence of cytochalasin D and stained for surface HA (green), actin (red–orange), and DNA (blue). A significant reduction in filamentous form and increase the spherical virion production was observed following treatment MDCK and CEF with the drug, while the infected DEF cells still produce short filaments (indicated by arrows). Scale bar 10 μm. (For interpretation of the references to color in this figure legend, the reader is referred to the web version of this article.)

co-localised with punctate aggregations of F-actin, as previously described (Simpson-Holley et al., 2002). These aggregations were more marked in MDCK and CEFs than DEFs. Although the use of a high dose of cytochalasin D (5 μg/ml) showed cell rounding and actin collapse following the inhibition of duck cells, short filaments were still produced (data not shown), suggesting that although the actin cytoskeleton promotes filamentous virus formation, other cellular factors also contribute.

Although fibroblasts are not typical host cells for influenza virus replication *in vivo*, primary fibroblasts derived from avian embryos are commonly used for culture and assay of avian influenza viruses. The morphological differences between influenza A H1N1 viruses A/Swine/Wisconsin/87/2005 (filamentous) and A/California/04/09 (spherical) were observed to be similar in both swine kidney fibroblast LLC-PK1 cells and human lung epithelial A549 cells, indicating that virion morphology is conserved between these cell types (Bialas et al., 2012). Despite this, future work should determine virus morphology in other relevant cell types such as duck and chicken epithelial cells.

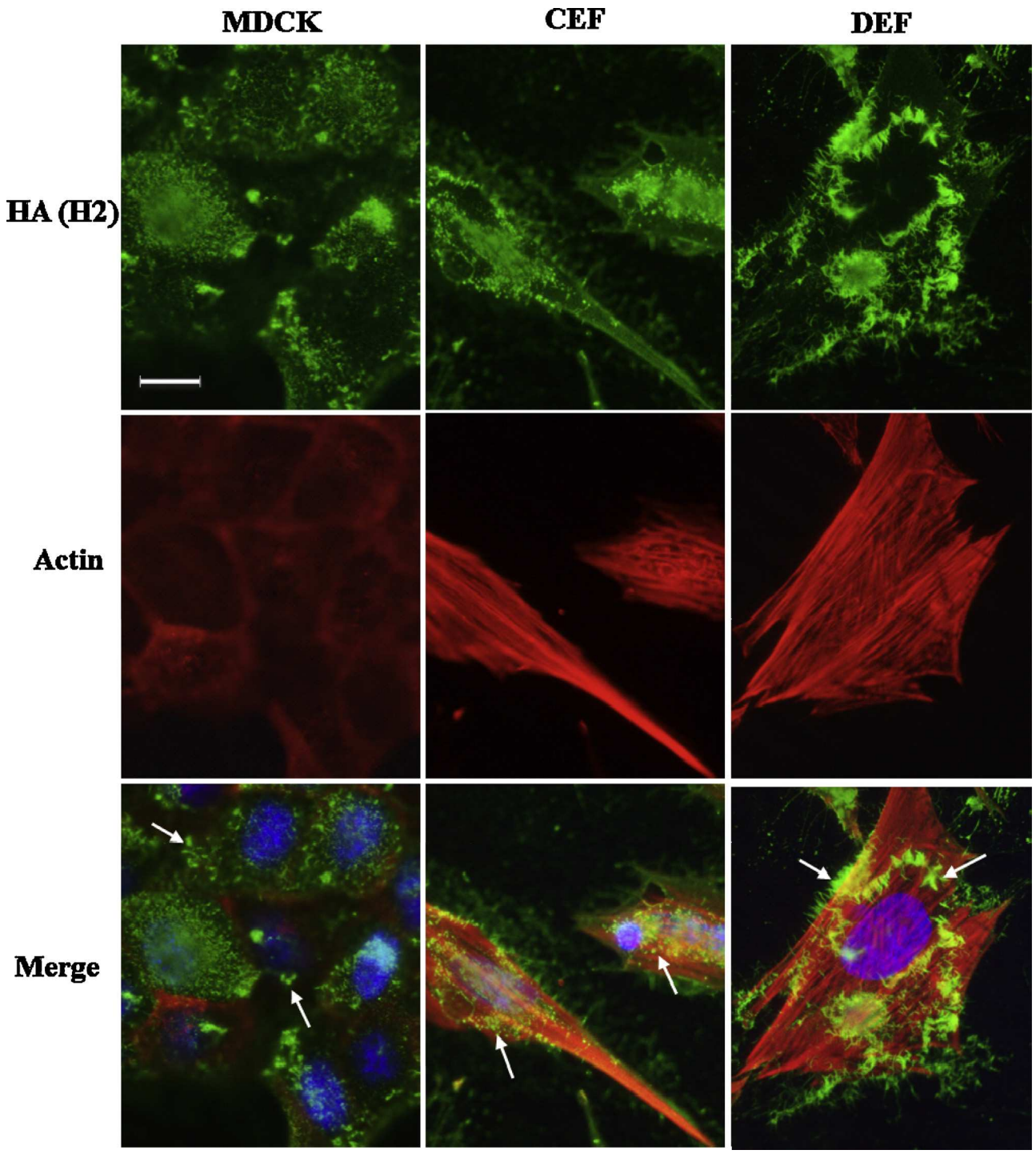

Fig. 7. H2N3 morphology in MDCK, CEF and DEF cells. Cells were infected with virus in the absence of cytochalasin D and stained for surface HA (green), actin (red–orange), and DNA (blue). Spherical virions were observed on the surface of MDCK and CEF cells, while short filaments were observed on the surface of DEF cells (indicated by arrows). Scale bar 10 μm. (For interpretation of the references to color in this figure legend, the reader is referred to the web version of this article.)

Cellular Rab11 (a small GTP-binding protein involved in endocytic recycling) and Rab11-family interacting protein 3 (FIP3), play a role in membrane trafficking and regulation of actin dynamics, in influenza virus budding and morphogenesis (Bruce et al., 2010). Both Rab11 and FIP3 proteins are required to support the formation of filamentous particles, while Rab11 is additionally involved in the final budding step of spherical virions. The expression and structure of these proteins in CEF and DEF cells and their impact on regulating influenza virus morphology have yet to be determined.

A recent study showed that autophagy, a cellular stress response that is induced by starvation or a range of other stressors, may be manipulated by the virus through the interaction of viral M2 with the essential autophagy protein LC3. This interaction apparently subverts autophagy to the benefit of the virus, providing suitable resources for viral budding and enhancing virion stability. This study also showed that mutations in M2 protein abolish LC3 binding, which results in reduced virion stability of filamentous influenza (Beale et al., 2014). We have observed that LC3 expression

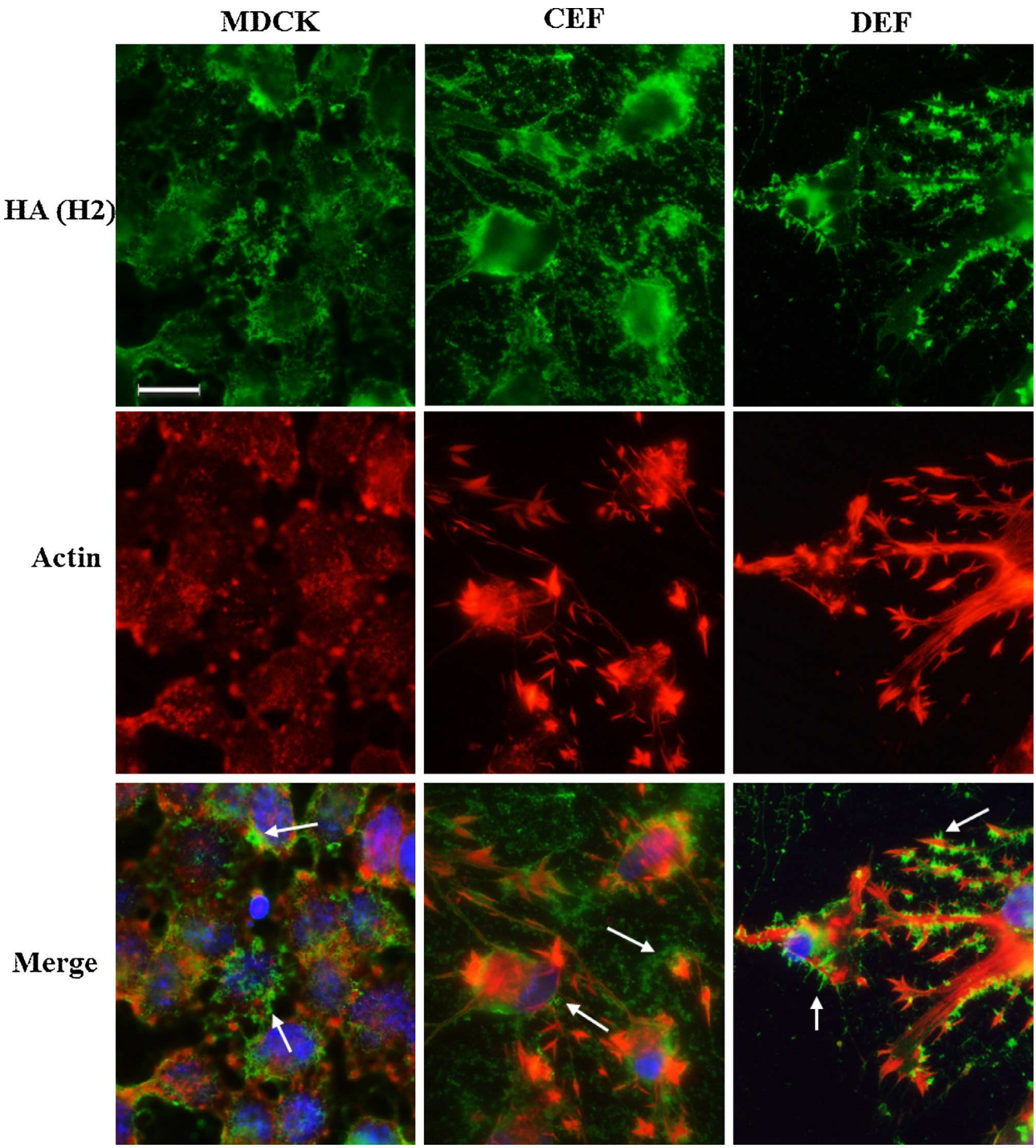

Fig. 8. Differences in H2N3 morphology between MDCK, CEF and DEF cells treated with cytochalasin D. Cells were infected with virus in the presence of cytochalasin D and stained for surface HA (green), actin (red–orange), and DNA (blue). Spherical virions were observed on the surface of MDCK and CEF cells, while elongated and short filaments were observed on the surface of DEF cells (indicated by arrows). Scale bar 10 μm. (For interpretation of the references to color in this figure legend, the reader is referred to the web version of this article.)

is significantly up-regulated in DEF cells, but not in CEF cells, following infection with H2N3 (unpublished data). This leads to the speculation that higher levels of LC3 in duck cells might support the release of short filament virions. Further study is required to study the effect of LC3 protein on the modulation of virus morphology. Multiple viral proteins including membrane proteins HA, NA and M2 are important in determining virus morphology (Jin et al., 1997; Zhang et al., 2000; Chen et al., 2008). It has been suggested that M1 interacts with HA and NA to stabilize the morphology of budding virus particles (Bialas et al., 2012). It seems plausible that the induction of autophagy by influenza A infection influences the interaction of multiple viral proteins, resulting in changes in virus assembly and consequently, virus morphology.

5. Conclusions

We have shown that virion morphology differs markedly between duck and chicken cells replicating H2N3 influenza. This

difference is unlikely to be due to viral factors. Although filament length in duck-grown viruses is somewhat affected by actin disruption, other host mechanisms, as yet undetermined, are likely to be involved. The observed difference in virus morphology may explain the reduced production of infectious virus from duck cells in comparison with chicken cells and could play a role in maintenance of virus in the natural reservoir host.

Acknowledgment

This work was supported by a PhD studentship funded by the Government of Iraq's Ministry of Higher Education and Scientific Research (ref. 1860/2010-509).

References

Beale, R., Wise, H., Stuart, A., Ravenhill, B.J., Digard, P., Randow, F., 2014. A LC3-interacting motif in the influenza a virus m2 protein is required to subvert autophagy and maintain virion stability. Cell Host Microbe 15, 239–247.

Bialas, K.M., Bussey, K.A., Stone, R.L., Takimoto, T., 2014. Specific nucleoprotein residues affect influenza virus morphology. J. Virol. 88, 2227–2234.

Bialas, K.M., Desmet, E.A., Takimoto, T., 2012. Specific residues in the 2009 H1N1 swine-origin influenza matrix protein influence virion morphology and efficiency of viral spread in vitro. PLoS ONE 7, e50595.

Bourmakina, S.V., Garcia-Sastre, A., 2003. Reverse genetics studies on the filamentous morphology of influenza A virus. J. Gen. Virol. 84, 517–527.

Bouvier, N.M., Palese, P., 2008. The biology of influenza viruses. Vaccine 26 (Suppl. 4), D49–D53.

Bruce, E.A., Digard, P., Stuart, A.D., 2010. The Rab11 pathway is required for influenza A virus budding and filament formation. J. Virol. 84, 5848–5859.

Bubb, M.R., Senderowicz, A.M., Sausville, E.A., Duncan, K.L., Korn, E.D., 1994. Jasplakinolide, a cytotoxic natural product, induces actin polymerization and competitively inhibits the binding of phalloidin to F-actin. J. Biol. Chem. 269, 14869–14871.

Burleigh, L.M., Calder, L.J., Skehel, J.J., Steinhauer, D.A., 2005. Influenza a viruses with mutations in the m1 helix six domain display a wide variety of morphological phenotypes. J. Virol. 79, 1262–1270.

Calder, L.J., Wasilewski, S., Berriman, J.A., Rosenthal, P.B., 2010. Structural organization of a filamentous influenza A virus. Proc. Natl. Acad. Sci. U. S. A. 107, 10685–10690.

Campbell, P.J., Danzy, S., Kyriakis, C.S., Deymier, M.J., Lowen, A.C., Steel, J., 2014a. The M segment of the 2009 pandemic influenza virus confers increased neuraminidase activity, filamentous morphology, and efficient contact transmissibility to A/Puerto Rico/8/1934-based reassortant viruses. J. Virol. 88, 3802–3814.

Campbell, P.J., Kyriakis, C.S., Marshall, N., Suppiah, S., Seladi-Schulman, J., Danzy, S., Lowen, A.C., Steel, J., 2014b. Residue 41 of the Eurasian avian-like swine influenza a virus matrix protein modulates virion filament length and efficiency of contact transmission. J. Virol. 88, 7569–7577.

Chen, B.J., Leser, G.P., Jackson, D., Lamb, R.A., 2008. The influenza virus M2 protein cytoplasmic tail interacts with the M1 protein and influences virus assembly at the site of virus budding. J. Virol. 82, 10059–10070.

Choppin, P.W., Murphy, J.S., Stoeckenius, W., 1961. The surface structure of influenza virus filaments. Virology 13, 548–550.

Chu, C.M., Dawson, I.M., Elford, W.J., 1949. Filamentous forms associated with newly isolated influenza virus. Lancet 1, 602.

Coue, M., Brenner, S.L., Spector, I., Korn, E.D., 1987. Inhibition of actin polymerization by latrunculin A. FEBS Lett. 213, 316–318.

Cox, J.C., Hampson, A.W., Hamilton, R.C., 1980. An immunofluorescence study of influenza virus filament formation. Arch. Virol. 63, 275–284.

Elleman, C.J., Barclay, W.S., 2004. The M1 matrix protein controls the filamentous phenotype of influenza A virus. Virology 321, 144–153.

Elton, D., Bruce, E.A., Bryant, N., Wise, H.M., Macrae, S., Rash, A., Smith, N., Turnbull, M.L., Medcalf, L., Daly, J.M., Digard, P., 2013. The genetics of virus particle shape in equine influenza A virus. Influenza Other Respir. Viruses 7 (Suppl. 4), 81–89.

Gomez-Puertas, P., Albo, C., Perez-Pastrana, E., Vivo, A., Portela, A., 2000. Influenza virus matrix protein is the major driving force in virus budding. J. Virol. 74, 11538–11547.

Holland, J.J., 1990. Defective viral genomes. Virology 1, 151–165.

Hughey, P.G., Roberts, P.C., Holsinger, L.J., Zebedee, S.L., Lamb, R.A., Compans, R.W., 1995. Effects of antibody to the influenza A virus M2 protein on M2 surface expression and virus assembly. Virology 212, 411–421.

Jeong, O.M., Kim, M.C., Kim, M.J., Kang, H.M., Kim, H.R., Kim, Y.J., Joh, S.J., Kwon, J.H., Lee, Y.J., 2009. Experimental infection of chickens, ducks and quails with the highly pathogenic H5N1 avian influenza virus. J. Vet. Sci. 10, 53–60.

Jin, H., Leser, G.P., Zhang, J., Lamb, R.A., 1997. Influenza virus hemagglutinin and neuraminidase cytoplasmic tails control particle shape. EMBO J. 16, 1236–1247.

Kilbourne, E.D., Murphy, J.S., 1960. Genetic studies of influenza viruses. I. Viral morphology and growth capacity as exchangeable genetic traits. Rapid in ovo adaptation of early passage Asian strain isolates by combination with PR8. J. Exp. Med. 111, 387–406.

Kishida, N., Sakoda, Y., Isoda, N., Matsuda, K., Eto, M., Sunaga, Y., Umemura, T., Kida, H., 2005. Pathogenicity of H5 influenza viruses for ducks. Arch. Virol. 150, 1383–1392.

Kuchipudi, S.V., Dunham, S.P., Nelli, R., White, G.A., Coward, V.J., Slomka, M.J., Brown, I.H., Chang, K.C., 2011. Rapid death of duck cells infected with influenza: a potential mechanism for host resistance to H5N1. Immunol. Cell Biol. 90, 116–123.

Latham, T., Galarza, J.M., 2001. Formation of wild-type and chimeric influenza virus-like particles following simultaneous expression of only four structural proteins. J. Virol. 75, 6154–6165.

Noda, T., 2011. Native morphology of influenza virions. Front. Microbiol. 2, 269.

Palese, P., Shaw, M.L., 2007. Orthomyxoviridae: the viruses and their replication. In: Knipe, D.M., Howley, P.M. (Eds.), Fields Virology, 5th. Lippincott Williams and Wilkins, Philadelphia, pp. 1647–1689.

Pillai, S.P., Pantin-Jackwood, M., Suarez, D.L., Saif, Y.M., Lee, C.W., 2010. Pathobiological characterization of low-pathogenicity H5 avian influenza viruses of diverse origins in chickens, ducks and turkeys. Arch. Virol. 155, 1439–1451.

Roberts, P.C., Compans, R.W., 1998. Host cell dependence of viral morphology. Proc. Natl. Acad. Sci. U. S. A. 95, 5746–5751.

Roberts, P.C., Lamb, R.A., Compans, R.W., 1998. The M1 and M2 proteins of influenza A virus are important determinants in filamentous particle formation. Virology 240, 127–137.

Schliwa, M., 1982. Action of cytochalasin D on cytoskeletal networks. J. Cell Biol. 92, 79–91.

Shortridge, K.F., Zhou, N.N., Guan, Y., Gao, P., Ito, T., Kawaoka, Y., Kodihalli, S., Krauss, S., Markwell, D., Murti, K.G., Norwood, M., Senne, D., Sims, L., Takada, A., Webster, R.G., 1998. Characterization of avian H5N1 influenza viruses from poultry in Hong Kong. Virology 252, 331–342.

Simpson-Holley, M., Ellis, D., Fisher, D., Elton, D., McCauley, J., Digard, P., 2002. A functional link between the actin cytoskeleton and lipid rafts during budding of filamentous influenza virions. Virology 301, 212–225.

Slomka, M.J., Pavlidis, T., Coward, V.J., Voermans, J., Koch, G., Hanna, A., Banks, J., Brown, I.H., 2009. Validated RealTime reverse transcriptase PCR methods for the diagnosis and pathotyping of Eurasian H7 avian influenza viruses. Influenza Other Respir. Viruses 3, 151–164.

Sugita, Y., Noda, T., Sagara, H., Kawaoka, Y., 2011. Ultracentrifugation deforms unfixed influenza A virions. J. Gen. Virol. 92, 2485–2493.

Sun, X., Whittaker, G.R., 2007. Role of the actin cytoskeleton during influenza virus internalization into polarized epithelial cells. Cell. Microbiol. 9, 1672–1682.

Webster, R.G., Bean, W.J., Gorman, O.T., Chambers, T.M., Kawaoka, Y., 1992. Evolution and ecology of influenza A viruses. Microbiol. Rev. 56, 152–179.

Webster, R.G., Yakhno, M., Hinshaw, V.S., Bean, W.J., Murti, K.G., 1978. Intestinal influenza: replication and characterization of influenza viruses in ducks. Virology 84, 268–278.

Zhang, J., Leser, G.P., Pekosz, A., Lamb, R.A., 2000. The cytoplasmic tails of the influenza virus spike glycoproteins are required for normal genome packaging. Virology 269, 325–334.